Theor Chim Acta (1992) 83: 21–30

Theoretica Chimica Acta

© Springer-Verlag 1992

A detailed analysis of pseudorotation in PH_4F*

Theresa L. Windus and Mark S. Gordon
Department of Chemistry, North Dakota State University, Fargo, ND 58105, USA

Received April 22, 1991/Accepted September 17, 1991

Summary. Pentacoordinated molecules are thought to undergo intramolecular isomerization by the widely accepted Berry pseudorotation mechanism. Through our investigations, we have found that the actual pseudorotation for the PH_4F system is more complex than that envisioned by Berry. The potential energy surface of PH_4F is mapped out at the RHF/6-311G(*d*, *p*) level. According to the Berry mechanism, this system is expected to have two minima and two maxima; however, the system actually has two transition states and one global minimum. The minimum energy path from the highest transition state is followed to the second transition state, which in turn has a minimum energy path leading to the global minimum. Along the path between the two transition states there is a branching region. This portion of the potential energy surface is probed extensively.

Key words: PH_4F – Pentacoordinated molecules – Pseudorotation

1 Introduction

The reactivity of pentacoordinated compounds, particularly those with silicon or phosphorus centers, is profoundly influenced by the orientational preferences and motions about the central atom. For pentacoordinated compounds with a trigonal bipyramidal structure, Berry [1] proposed that conformational changes occur via a square pyramidal transition state, as illustrated in Fig. 1. This mechanism, termed Berry pseudorotation, was explicitly demonstrated for SiH_5^- by tracing the minimum energy path (MEP) connecting the two equivalent trigonal bipyramidal minima [2].

When the central atom is surrounded by two or more *different* ligands, it is generally accepted that several minima exist, such that each ligand can be placed in either an axial or an equatorial position. Thus, for a compound AH_4X, one expects to find four stationary points: two minima with X either axial (**1**) or

* Dedicated to Prof. Klaus Ruedenberg

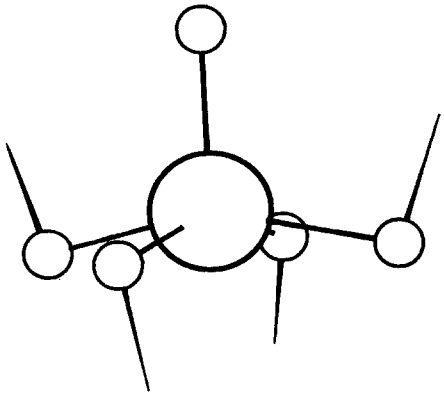

Fig. 1. Imaginary normal mode for square pyramidal SiH_5^-

equatorial (**2**) and two square pyramidal transition states with X either basal (**3**) or apical (**4**). However, it has already been demonstrated [3] that in the case of SiH_4F^-, structures **2** and **3** merge into a single transition state, leaving only one minimum (**1**) on the conformational potential energy surface, if an adequate level of theory is used (i.e. RHF/6-31++G(*d*, *p*)). Since the minimum energy, steepest descent path leading from **4** (F apical) to **2** (F equatorial) connects two transition states (i.e., two structures, each of which has one imaginary frequency corresponding to a downhill motion), it was suggested that (a) the pseudorotational "mechanism" in compounds such as SiH_4F^- can be more complex than that envisioned in the Berry mechanism and (b) a bifurcation is to be expected along the MEP.

The molecule PH_4F is isoelectronic with SiH_4F^- and is a simple pentacoordinated phosphorus compound which is expected to have two minimum energy structures (**1** and **2**) on its ground state conformational potential energy surface (PES). In the present paper, the conformational PES of PH_4F is explored in detail in an attempt to understand the complex nature of its pseudorotational mechanism.

While PH_4F is as yet unknown experimentally, there have been several *ab initio* studies of the species suggesting that PH_4F is a minimum on the PES. Several of these investigations [4] were limited to the structure with F in the axial position. Stritch and Veillard [5], using idealized geometries, predicted the equatorial (**2**) and square pyramidal (**3**) structures to be 15.8 and 7.9 kcal/mol above the axial structure (**1**). Keil and Kutzelnigg [6], using constrained geometry optimizations, found the equatorial structure to be 23 kcal/mol above axial. McDowell and Streitweiser [7] performed geometry optimizations and predicted equatorial PH_4F to be 7.5 kcal/mol above axial, but no Hessians were evaluated to assess the nature of the stationary points. Most recently, Wang et al. [8] carried out full geometry optimizations for the axial, equatorial, and square pyramidal structures for several PH_4X compounds. For X = F, these authors found the equatorial structure to be a transition state 8.0 kcal/mol above axial. The square pyramidal structure with F in the apical position (**4**) was predicted to be 33.5 kcal/mol above axial. While the reactions $PH_4F \rightarrow PH_3 + HF$ and $PH_4F \rightarrow PH_2F + H_2$ are exothermic (16.2 and 4.1 kcal/mol, respectively, at the MP2/6-311G(*d*, *p*)//MP2/6-311G(*d*, *p*) level of theory), it is nonetheless a minimum on the potential energy surface and therefore of interest from the point of view of pseudorotation.

2 Computational approach

In order to determine the dependence of the calculated energetics and stationary points on the level of theory, the structures of all stationary points were determined at several levels. The simplest level of theory used (referred to as Level A) is the self-consistent field (SCF) method with the 6-31G(*d*) [9] basis set. In Level B, the structures are again determined with SCF wavefunctions, but with the larger 6-311G(*d*, *p*) [10] basis set. Finally, in Level C the 6-311G(*d*, *p*) basis is used in conjunction with second order Moller–Plesset perturbation theory [11]. All stationary points were characterized as minima or transition states by calculating and diagonalizing the matrix of energy second derivatives (Hessian) to determine the number of negative force constants (0 for minima, 1 for transition states).

To follow each minimum energy path (MEP), the fourth order Runge–Kutta (RK4) and the Euler with stabilization (ES2) algorithms, developed in this laboratory [12], were used with step sizes varying from 0.0001 to 0.05 bohr-amu$^{1/2}$ depending on the convergence of the paths. All MEP's were calculated at Level B.

The projection method of Miller, Handy, and Adams [13], which projects out the translations, rotations and gradient at non-stationary points, was used to analyze the frequencies along the MEP's. In addition, the purification method developed in this laboratory [14] was used to obtain qualitative information about the frequencies associated with the reaction path (see Appendix). The purification method removes the rotations and translations from the vibrations. This method provides only qualitative results, since the gradient is not projected out. So, the eigenvalues of this purified but unprojected Hessian can be used to obtain frequencies only when the gradient is small.

All calculations were performed using the electronic structure theory code GAMESS [15] and a locally modified version of GAUSSIAN86 [16].

3 Results and discussion

3.1 Structures and energetics

At all levels of theory used in this work, only three stationary points are found on the PH_4F PES. The axial structure **1** is predicted to be a minimum, while the equatorial (**2**) and apical (**4**) structures are found to be transition states. Thus, in analogy with the previous calculations on SiH_4F^- [3], the basal structure **3** merges with **2**, and there is a minimum energy path connecting two transition states **2** and **4**. An important difference between PH_4F and SiH_4F^- is that in the former molecule the equatorial structure is clearly a transition state even at the SCF/6-31G(*d*) level of theory. The imaginary frequency in the equatorial structure is calculated to be 261*i*, 324*i*, and 298*i* cm^{-1} according to Levels A, B, and C, respectively. The corresponding values for the apical structure are 1067*i*, 1031*i*, and 1084*i* cm^{-1}, respectively.

The structures of the three stationary points are illustrated in Fig. 2, and the energetics are summarized in Table 1. The structures follow the generally expected trends. The axial bonds are somewhat longer than the equatorial bonds for both ligands, since the axial atoms are bound by a three-center, four-electron bond. The apical PF bond is even shorter than that in the equatorial structure.

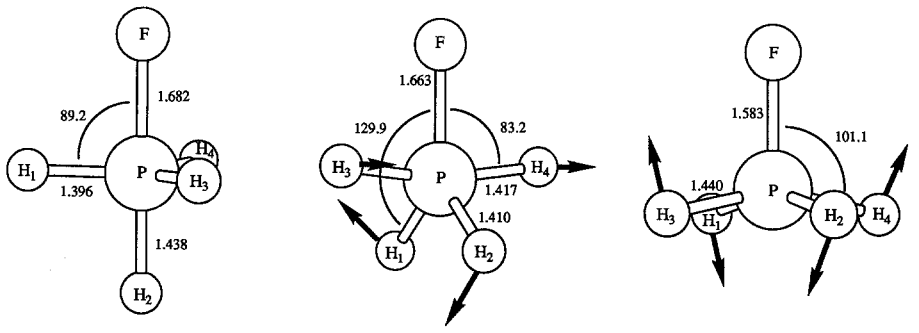

Fig. 2. MP2/6-311G(*d*, *p*) structures. Imaginary frequencies in cm^{-1} are given for transition states. Bond lengths are in Ångstroms and bond angles are in degrees

Table 1. Total (hartree) and relative[a] energies (kcal/mol) for PH_4F isomers

Level	Axial	Equatorial	Apical
A	−442.43020 (0.0)	−442.41264 (11.0)	−442.37744 (33.1)
B	−442.49316 (0.0)	−442.47829 (9.3)	−442.43822 (34.5)
C	−442.91968 (0.0)	−442.90455 (9.5)	−442.86447 (34.6)

[a] Energies relative to the axial isomer are given in parentheses

The effects of both basis set and correlation on the calculated geometries are small, with the largest change being the 0.03 Å increase in the equatorial PF bond length upon the addition of correlation.

Improving the basis set from 6-31G(*d*) to 6-311G(*d*, *p*) decreases the axial-equatorial energy difference (Table 1) by 1.7 kcal/mol and increases the axial-apical energy difference by 1.4 kcal/mol. Both of these energy differences are somewhat larger than those found for SiH_4F^-. The addition of correlation has virtually no effect on the calculated relative energies. The addition of zero point vibrational energies changes the results in Table 1 by less than 1 kcal/mol in all cases.

The normal modes for the transition states (TS's) are shown in Fig. 2. The normal mode for **4** shows this to be the TS for the Berry pseudorotation connecting two equivalent equatorial structures (**2**→**2**). However, **2** is itself a TS which connects two equivalent axial structures (**1**→**1**). To illustrate, the normal mode of **2** demonstrates that H_2 and F are moving into axial positions and H_1, H_3, and H_4 are moving into equatorial positions, giving isomer **1**. Indeed, the mode shown for **2** in Fig. 2 is strikingly similar (although not identical) to the turnstile TS discussed by several authors [17]. The difference is that one does not expect the turnstile TS to occur at what is essentially the equatorial structure. Therefore, it is of interest to explore the MEP's that connect the stationary structures to determine the nature of the potential energy surface.

When two TS's are connected by a MEP, either a bifurcation or a branching region must occur, because a second imaginary frequency associated with the lower energy TS is building in somewhere along the path. This second imaginary frequency (which indicates that the molecule may follow a motion not dictated by the MEP) is not "recognized" by the MEP. This is because the MEP by

definition follows the steepest descent (gradient) path and therefore may not break symmetry. A bifurcation is identified by two imaginary frequencies, one associated with each TS, in the same region. In a branching region, the first imaginary frequency (associated with the higher energy TS) becomes real before the second imaginary frequency (associated with the lower energy TS) builds in. In either case (bifurcation or branching), a molecule not constrained by symmetry may move away from the MEP when it encounters a new imaginary mode. As will be discussed below, a branching region occurs in the PH_4F pseudorotation reaction.

3.2 MEP's and branching region

To examine this surface, the MEP's from **4** and **2** were calculated using the methods mentioned in Sect. 2. The MEP's that connect structures **4** and **2** and structures **2** and **1** are displayed in Figs. 3 and 4, respectively. These will be referred to as MEP4 → 2 and MEP2 → 1, respectively. MEP2 → 1 is relatively flat at the beginning. This prompted the use of very small step sizes to obtain path convergence. This is in contrast to MEP4 → 2 where the surface is not very flat and larger step sizes could be used.

Since a MEP follows the gradient and the gradient is totally symmetric in both cases, the MEP retains the symmetry of the molecule. So, MEP4 → 2 is a C_{2v} path and therefore leads directly to **2**. However, since there must be a bifurcation or branching somewhere on the MEP, the molecule need not be constrained to C_{2v} symmetry; that is, it may leave the original MEP.

To discover the point on MEP4 → 2 at which the new imaginary mode first appears, force fields were calculated at several points along this path. Figure 5 is a plot of the projected normal modes along MEP4 → 2. The lowest A_1 frequency (the one associated with MEP4 → 2) is projected to zero by the projection scheme and therefore the data for this frequency is obtained through the purification method. The frequency for the lowest A_1 mode goes from imaginary at small s to 0 between $s = 0.952$ and $s = 1.052$ bohr-amu$^{1/2}$ to positive for large s. Also, by examining the lowest B_2 mode (this is the mode initially followed for MEP2 → 1), the associated frequency goes from positive at small s to 0 between $s = 1.962$ and

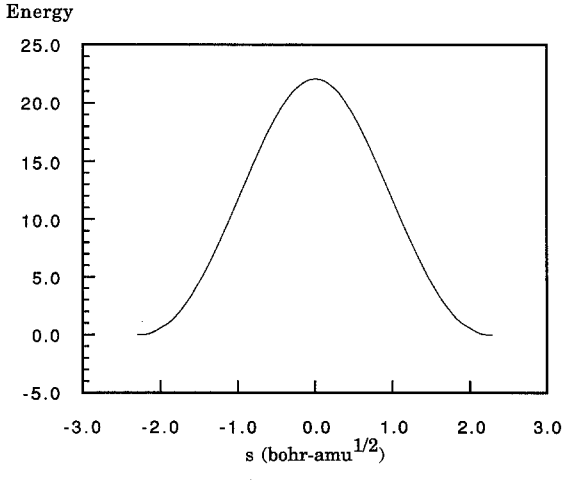

Fig. 3. PH_4F IRC from F apical, tetragonal, energy vs. reaction coordinate, energy is relative to structure 2; energy unit is kcal/mol

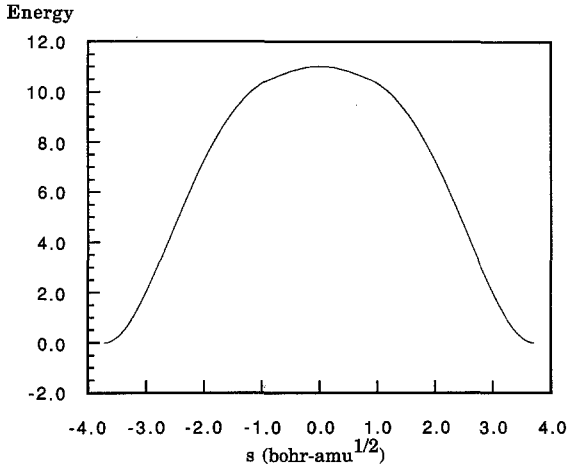

Fig. 4. PH_4F IRC from F equatorial, trigonal bipyramidal, energy vs. reaction coordinate, energy unit is kcal/mol

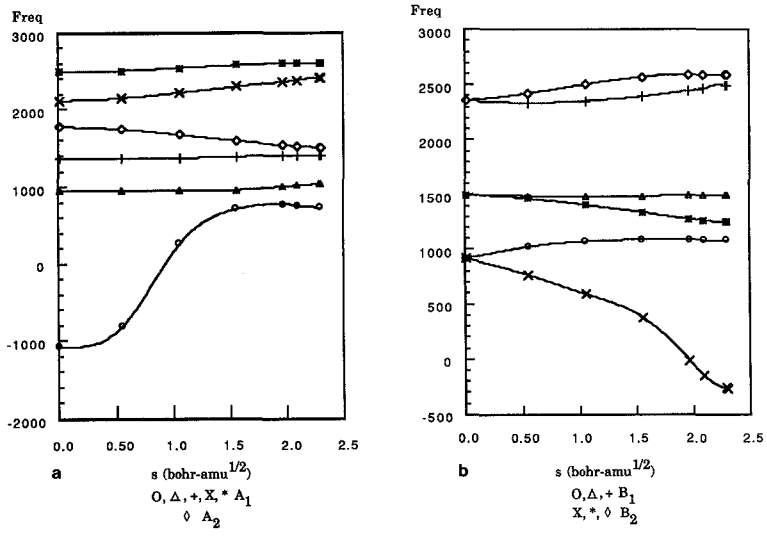

Fig. 5. a. PH_4F pseudorotation from C_{4v} structure generalized harmonic frequencies – A_1 and A_2 generalized normal models; **b.** PH_4F pseudorotation from C_{4v} structure generalized harmonic frequencies – B_1 and B_2 generalized normal modes

$s = 1.963$ bohr-amu$^{1/2}$ to imaginary for large s. By comparing the s values at which the two frequencies become zero, we see that the A_1 frequency becomes zero (has an inflection point) before the B_2 frequency becomes imaginary. At the point that the B_2 frequency becomes zero there is a branching point. As discussed by Ruedenberg [18] and others [19], the downhill path from **4** can proceed to **1** without passing through **2**. In other words, the reaction could continue to follow MEP4 → 2, follow the direction associated with the B_2 mode, or some composite of the two. In reality, the amount of energy available to the system (e.g., the temperature) will play a role in the actual **motion**.

In an attempt to further explore the branching region between $s = 1.962$ and $s = 2.298$, "jumps" were taken off of MEP4 → 2 in the direction dictated by the

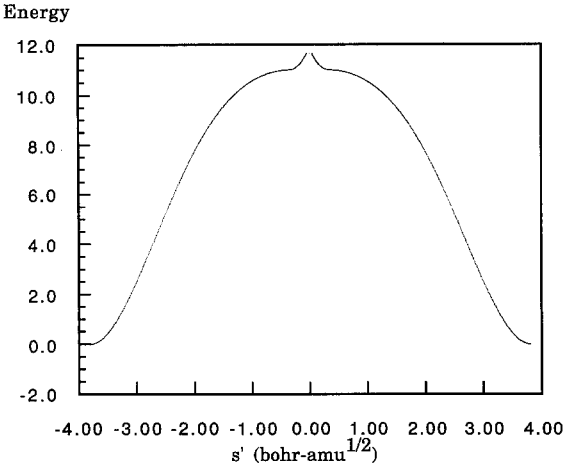

Fig. 6. PH_4F IRC from $s = 1.963$ bohr-amu$^{1/2}$, energy vs. reaction coordinate; energy unit is kcal/mol

B_2 mode for several points in this region, and then the gradient was followed to the minimum structure, **1**. For clarity, these jumping off points will be referred to as "path initiation points" (PIP's) and the MEP's from the PIP's will be referred to as "branching paths" (BP's). The resulting plots of energy vs. reaction coordinate for $s = 1.963$, 1.985, 2.086, and 2.286 bohr-amu$^{1/2}$ are given in Figs. 6, 7, 8, and 9, respectively. The projected B_2 frequencies associated with these points are $15.3i$, $82.0i$, $149.1i$, and $259.7i$ cm^{-1}, respectively. The magnitudes of these frequencies suggest that the surface associated with the B_2 mode starts out rather flat and gradually gains more curvature as the molecule progresses farther along the branching region.

Several comments need to be made about Figs. 6–9. First, these plots have an unusual shape at the top of the BP. This can be explained in the following manner. The initial step from the PIP's were taken such that the energy would decrease by less than 1×10^{-5} au. In cases where the surface is very flat this first step can still be quite large. The large step with small energy decrease accounts

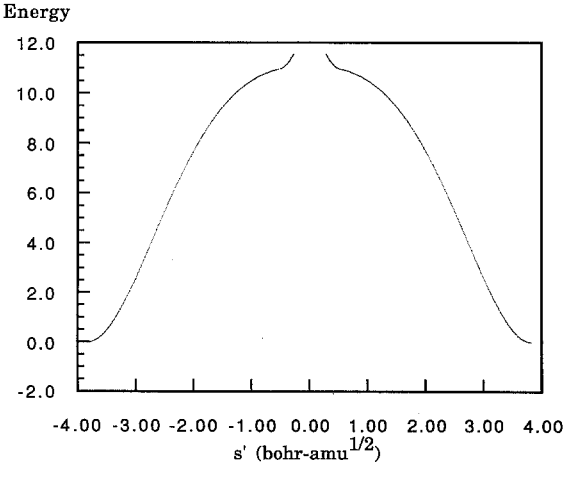

Fig. 7. PH_4F IRC from $s = 1.985$ bohr-amu$^{1/2}$, energy vs. reaction coordinate; energy unit is kcal/mol

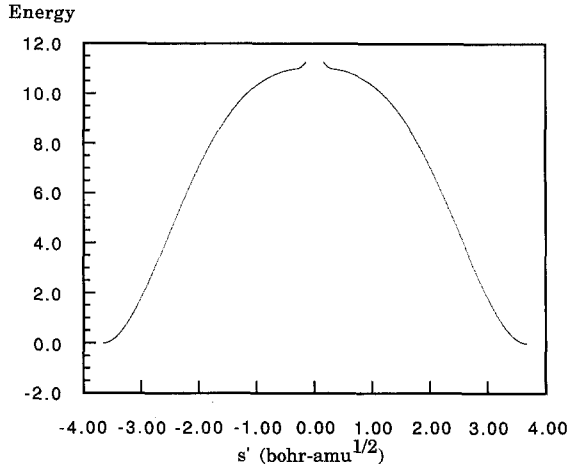

Fig. 8. PH_4F IRC from $s = 2.086$ bohr-amu$^{1/2}$, energy vs. reaction coordinate; energy unit is kcal/mol

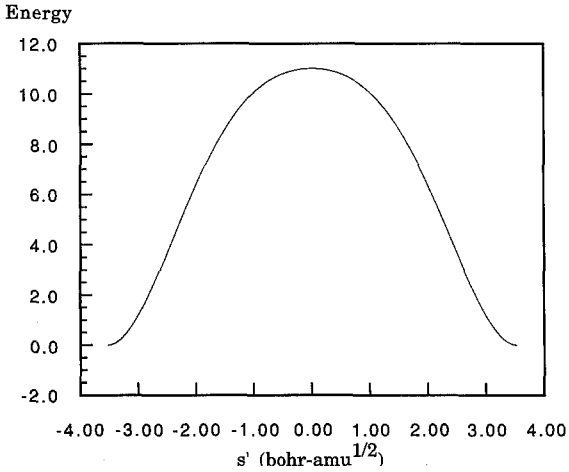

Fig. 9. PH_4F IRC from $s = 2.286$ bohr-amu$^{1/2}$, energy vs. reaction coordinate; energy unit is kcal/mol

for the singularities at $s' = 0.0$ in Figs. 6, 7, and 8 [20]. Also, the resulting gradient of the initial step from the PIP is only slightly changed from the gradient of the PIP. As the molecule follows the BP, the gradient is changing from a gradient similar to MEP4 → 2 to that of a gradient similar to MEP2 → 1; until finally, the gradient is essentially that of MEP2 → 1. This change in the nature of the gradient, and therefore the potential energy surface, is directly seen in Figs. 6, 7, and 8. The initial points along the BP (those following a gradient similar to MEP4 → 2) are following a faster changing portion of the surface than are the points after the gradient has changed to that of MEP2 → 1. Therefore, we see a characteristic change in the curvature of the plots.

Second, since the molecules tend to have gradients similar to MEP4 → 2 at the beginning of the BP and to have gradients similar to MEP2 → 1 after only a drop of less than one kcal/mol, the molecule must stay in a reaction swath that is rather narrow. The fact that the branching point is close to **2** also suggests that the branching region of the surface must span a small volume near MEP4 → 2 and MEP2 → 1. This implies that while the reaction may not go exactly through

2, it will come close to **2**. This could have interesting effects on the dynamics of this system.

As a final point, the "bump" in the BP's starts to become smaller and flatten out as we start at PIP's farther along MEP4 → 2, until at PIP's close to **2** it is essentially gone. Figure 9, which is a BP from a structure close to that of **2**, bears this out. This trend is to be expected. The further along MEP4 → 2 the molecule is before it takes its "jump", the more the gradient of the molecule is going to resemble that of MEP2 → 1. In other words, at the initial step from $s = 1.963$ bohr-amu$^{1/2}$ the gradient is more like that of MEP4 → 2 than the initial step from $s = 1.985$ bohr-amu$^{1/2}$. The latter is more of a composite of the gradients for MEP4 → 2 and MEP2 → 1. Also, if the molecule is starting at a lower energy on MEP4 → 2 it has less of the reaction swath to follow than if it had "jumped" from a point of higher energy.

4 Conclusions

The results reported here have shown that the simple Berry pseudorotational model is not followed in the case of PH_4F. In fact, we obtain two maxima and one minimum as opposed to the two maxima and two minima that are expected. The pseudorotational path is that of **1** ⇔ **2** ⇔ **4** with a branching region occurring between **2** and **4**. In the narrow branching region, the molecule can proceed from **4** to **1** without going through **2**. As shown by the BP's from this region, the molecule will stay close to MEP4 → 2 and MEP2 → 1, but does not necessarily need to be on these paths. While these results are interesting in their own right, an analysis of the dynamics of this system is needed to fully understand this complex reaction. This will be reported in a later paper.

Acknowledgements. This work was supported by grants from the Air Force Office of Scientific Research (90-0052) and the Petroleum Research Fund, administered by the American Chemical Society. Calculations were performed on a DECstation 3100 and an IBM RS 6000/530, both obtained with the assistance of grants from AFOSR. Many helpful discussions with Drs. Michael Schmidt, Larry Davis, and Larry Burggraf are gratefully acknowledged.

Appendix

To convert from cartesian coordinate space to internal coordinate space one uses a $\boldsymbol{B}$ matrix such that:

$$r_i = \sum_j B_{ij} x_j.$$

This $\boldsymbol{B}$ matrix is formally defined as a $m \times 3N$ ($m = 3N - 6$ for nonlinear or $3N - 5$ for linear molecules) matrix where N is the number of atoms in the system. In practice, however, $\boldsymbol{B}$ is a square matrix [21]. This allows $\boldsymbol{B}$ to be inverted so we can also convert from internal coordinate space to cartesian coordinate space. Therefore, a cartesian Hessian matrix is converted to an internal Hessian matrix using:

$$h_r = (B^{-1})^t h_x B^{-1}$$

and also an internal Hessian matrix is converted to a cartesian Hessian matrix using:

$$B^t h_r B = h_x.$$

Formally, the internal Hessian matrix should be $m \times m$, but in practice, because the $\boldsymbol{B}$ matrix is square, the internal Hessian matrix is $3N \times 3N$. The extra elements in the matrix are associated with the rotations and translations, and should be exactly zero, but quite often are not. In the purification method, these very small non-zero elements are made to be exactly zero. Then, when the internal Hessian matrix is converted back to the cartesian Hessian matrix, the five or six frequencies associated with the rotations and translations are zero. In effect, the purification separates the rotations and translations from the vibrations.

References

1. Berry RS (1960) J Chem Phys 32:933
   Mislow K (1970) Acc Chem Res 3:321
2. Gordon MS, Windus TL, Burggraf LW, Davis LP (1990) J Am Chem Soc 112:7167
3. Windus TL, Gordon MS, Burggraf LW, Davis LP, J Am Chem Soc 113:4346
4. Deiters JA, Holmes RR (1990) J Am Chem Soc 112:7197
   Magnusson E (1990) J Am Chem Soc 112:7940
   Breidung J, Thiel W, Kormornicki A (1988) J Phys Chem 92:5603
5. Strich A, Veillard A (1973) J Am Chem Soc 95:5574
6. Keil F, Kutzelnigg W (1975) J Am Chem Soc 97:3623
7. McDowell RS, Streitwieser A Jr (1985) J Am Chem Soc 107:5849
8. Wang P, Zhang Y, Glaser R, Reed AE, Schleyer PvR, Streitwieser A (1991) J Am Chem Soc 113:55
9. Francl MM, Pietro WJ, Hehre WJ, Binkley JS, Gordon MS, DeFrees DJ, Pople JA (1982) J Chem Phys 77:3654
   Hehre WJ, Ditchfield R, Pople JA (1972) J Chem Phys 56:2257
   Ditchfield R, Hehre WJ, Pople JA (1971) J Chem Phys 54:724
   Hariharan PC, Pople JA (1973) Theor Chim Acta 28:213
10. Krishnan R, Binkley JS, Steeger R, Pople JA (1980) J Chem Phys 72:650
    McLean AD, Chandler GS (1980) J Chem Phys 72:5639
11. Pople JA, Binkley JS, Seeger R (1976) Int J Quantum Chem S10:1
12. Baldridge KK, Gordon MS, Steckler R, Truhlar DG (1989) J Phys Chem 93:5107
13. Miller WH, Handy NC, Adams JE (1980) J Chem Phys 72:99
14. Boatz JA, Schmidt MW implemented in GAMESS in 1986. See [15]
15. Schmidt MW, Baldridge KK, Boatz JA, Jensen JH, Koseki S, Gordon MS, Nguyen KA, Windus TL, Elbert ST (1990) QCPE Bull 10:52
16. Frisch MJ, Binkley JS, Schlegel HB, Raghavachari K, Melius CF, Martin RL, Stewart JJP, Bobrowicz FW, Rohlfing CM, Kahn LR, DeFrees DJ, Steeger R, Whiteside RA, Fox DJ, Fleuder EM, Pople JA Carnegie-Mellon Quantum Chemistry Publishing Unit Pittsburgh PA 15213
17. Ugi I, Ramirez F (1972) Chem Br 8:198
    Kutzelnigg W, Wasilewski J (1982) J Am Chem Soc 104:953
    Wang P, Argafiotis DK, Streitwieser A, Schleyer PvR (1990) J Chem Soc, Chem Comm 201
18. Hoffman DK, Nord RS, Ruedenberg K (1986) Theor Chim Acta 69:265
    Valtazanos P, Ruedenberg K (1986) Theor Chim Acta 69:281
19. Kraus WA, DePristo AE (1986) Theor Chim Acta 69:309
    Baker J, Gill PMW (1988) J Comp Chem 9:465
    Shida N, Almlöf JE, Barbara PF (1989) Theor Chim Acta 76:7
20. One of the reviewers has noted that an alternative explanation is "that the BP's, being non-symmetric, follow neither the downhill B_2 or A_1 modes per se, but must first jump over a small region of hypersurface which is higher in energy. Depending on the PIP, this may be a small or a large first step."
21. Wilson EB, Jr., Decius JC, Cross PC (1955) Molecular Vibrations, McGraw-Hill, New York Toronto London